INFLUENCE OF WORKING ATMOSPHERE COMPOSITION ON PLASMA NITRIDED LAYER CONSTITUTION

Sorin CIUCĂ[1], Mihai Ovidiu COJOCARU[1], Mirela Gabriela SOHACIU[1], Gabriel George GRIGORESCU[1], Ruxandra Elena DUMITRESCU[1*], Ioana Arina GHERGHESCU[1*]

Two steels belonging to the "Steels for quenching and tempering"class (EN 10083): C45 and 42CrMo4, were plasma nitrided under identical temperature conditions (T_N = 570°C) and several atmosphere chemical compositions. The structural investigation was carried out by optical microscopy, scanning electron microscopy and X-ray diffraction, while the chemical composition on the layer depth was conducted by Glow Discharge Mass Spectrometry. Low nitrogen content in the working chamber (5%N_2+95%H_2) completely suppresses the compounds layer formation, while an average nitrogen content (20...30%N_2 + 80 ... 70%H_2) facilitates the formation of a mainly γ' structure. Contrariwise, a high nitrogen content (80%N_2+20%H_2) allows a biphasic ε + γ' compound layer (prevailingly ε) to form. One may observe that by plasma nitriding a layer formed exclusively by ε phase can never be obtained. Adding to the first atmosphere a small proportion of carbon component gas (80%N_2 + 19.5%H_2 + 0.5%CH_4) makes possible to obtain a layer consisting in two subzones, the external one as an ε and the internal one as a γ' structure. A complete ε structure of the layer could be achieved only by plasma nitrocarburizing, but it is necessary to carefully measure the optimal methane content. The diffusion zone is less influenced by the nitriding technique (plasma or gaseous), being formed under constant nitrogen activity conditions, directly dependent on its diffusive transfer.

Keywords: plasma nitriding, atmosphere composition, carbon and nitrogen layer distribution

1. Introduction

The combined action of the phenomena taking place in the plasma as active environment, at the separation surface between the plasma and the metallic material and then inside it, materializes in the mechanisms that contribute to the ion nitrided layers formation. A significant importance on the structure, but also on the structural and dimensional uniformity of the ion nitrided layer, have the chemical (composition and especially the gas pressure in the working chamber) and electrical (voltage and intensity of the discharge current) parameters.

[1] Materials Science and Engineering Faculty, University POLITEHNICA of Bucharest, Romania
*Corresponding authors' e-mails: ioanaarinagherghescu@gmail.com; ruxandraelenadumitrescu@gmail.com

Their interdependence, by their influence on the reactions' chemistry in the discharge area adjacent to the cathode, ensures a particular temperature value [1].

As against the classic heating processes from an external source (by convection or radiation - the case of gaseous nitriding) [2] or an internal one (by conduction - the case of salt baths heating), the heating of the parts (in fact the cathode) in the luminescent discharge plasma occurs after the bombardment of positive ions, especially the NH, NH_2, NH_3 radicals, accelerated in the cathode discharge area [3].

2. Materials and Methods

The tested materials were two steels belonging to the class "Steels for quenching and tempering" (EN 10083): C45 and 42CrMo4. The selection criteria were:

- to have a carbon steel and an alloy steel of the same category;
- their carbon contents should have close values.

The experimental program, grouped in REGIMES 1, 2 and 3 had as research objective to establish the nitriding atmosphere chemical composition influence on the mechanisms that generates the layer's phasic nature. Thus, the working atmosphere composition was considered as a process variable, while constant parameters were the nitriding temperature and the holding time. In order to have the fastest formation layer'skinetics, the chosen temperature was towards the upper range limit, i.e. T_N = 570°C.

The applied nitriding regimes were the following:

- Regime 1 – regime signification – plasma nitriding: T_N = 570°C; t_{hold} = 6h; atmosphere composition: 25%N_2+75%H_2; p_{tot} = 1,8 torr.

By applying this regime, the aim was to obtain a (mostly) single phase γ' structure in the compounds area.

- Regime 2 – regime signification – plasma nitriding: T_N = 570°C; t_{hold} = 6h; atmosphere composition: 80%N_2+20%H_2; p_{tot} = 4 torr.

By experimenting this regime, the influence exerted by the nitrogen content increase in the working atmosphere on the ε phase formation in the compounds area was investigated.

- Regime 3 – regime signification – plasma nitrocarburizing: T_N = 570°C; t_{hold} = 9h; atmosphere composition: 80%N_2+19.5%H_2+0.5%CH_4 ; p_{tot} = 3 torr.

The main objective of the regime 3 was to obtain an ε single-phase structure in the compounds area. The carbon content favors the formation of this phase - the existence domain of ε carbonitride widens, the γ' (carbo)nitride narrows. Thermodynamic conditions are created for the nitrided layer to be composed of a single-phase ε compound zone and a diffusion zone.

The regimes experienced according to the established work program had the following research objectives:

- identifying the mechanisms by which the chemical composition of the atmosphere contributes to the realization of the compound area phase structure;
- identifying the mechanisms that appear along the diffusion zone formation;
- identifying the role of hydrogen in the ionic mechanism of nitrogen adsorption.

The three regimes were applied to samples C (C45) and E (42CrMo4).

3. Results and discussion

3.1. Determination of microhardness profiles and actual layers thickness

The first step of evaluating the nitriding results is to determine the microhardness distribution along the layers depth, associated with the determination of the actual layer thickness. The data resulting from the microhardness analysis are presented in Table 1.

Table 1

The nitrided layer depth and the maximum and minimum values of microhardness obtained for samples C and E nitrided according to regimes 1 - 3

Regimes	**Material sample codification**	**Layer characteristics**		
		White layer thickness, δ_C	Nitrided layer thickness, δ_N	Microhardness interval
Regime 1 (plasma nitriding) T_N = 570°C; t_{hold} =6h; atmosphere: 25%N_2 + 75%H_2; p_{tot} = 1,8 torr	C45 **C1**	γ'+(ε) δ_C = 8...10μm	δ_N = 301μm	450...278 μHV
	42CrMo4 **E1**	γ'+(ε) δ_C=8 μm	δ_N=289 μm	619...348 μHV
Regime 2 (plasma nitriding) T_N=570°C; t_{hold} =6h; atmosphere: 80%N_2 + 20%H_2; p_{tot} = 4torr	C45 **C2**	ε+(γ') δ_C=15 μm	δ_N=310 μm	454...284 μHV
	42CrMo4 **E2**	ε+(γ') δ_C=13...14 μm	δ_N=298 μm	672...359 μHV
Regime 3 (plasma nitrocarburizing) T_N=570°C; t_{hold} =9h; atmosphere: 80%N_2 + 19,5%H_2 + 0,5%CH_4; p_{tot}=3torr	C45 **C3**	ε+(γ') δ_C=23...25 μm δ_ε=15 μm $\delta_{\gamma'}$=10 μm	δ_N=325 μm	528...272 μHV
	42CrMo4 **E3**	ε+(γ') δ_C=20 μm δ_ε=14 μm $\delta_{\gamma'}$=6 μm	δ_N=302 μm	725...348 μHV

For the actual layer thicknesses, one observation is related to the influence of the atmosphere chemical composition on these values. Thus, for the same thermal and time parameters, but using atmospheres of different compositions

(Regime 1 - ratio N_2/H_2 = 1/3; Regime 2 - ratio N_2/H_2 = 4/1), the layer thicknesses also exhibit slightly different values.

Table 2

Layer thickness values for regimes 1 and 2

Regime 1 (25%N_2+75%H_2)	**Regime 2** (80%N_2+20%H_2)
samples C (C45) δ_N = 301 μm; δ_C = 8...10 μm	δ_N = 310 μm; δ_C = 15 μm
samples E (42CrMo4) δ_N = 289 μm; δ_C= 8 μm	δ_N= 298 μm; δ_C = 13...14 μm

Therefore, the more reactive the plasma, the higher the layer depths. The same is noted for the compound area thickness.

- The presence of carbon in a rich-nitrogen atmosphere, but also associated with the prolongation of the holding time (regime 3), favors obtaining a greater thickness compound area (δ_C > 25 μm). By means of optical microscopy techniques it was possible to make a separation between the two ε and γ' compounds of the white layer. It is found that, for the same working conditions, the layer subzone of structural compounds ε has an almost identical value for both experienced materials. For the alloy steel the subzone corresponding to the phase γ' is narrower. Thus:

$$[\delta_\varepsilon]_{C45} \cong 15\ \mu m, \text{ respectively } [\delta_\varepsilon]_{42CrMo4} \cong 14...15\ \mu m$$

$$[\delta_{\gamma'}]_{C45} \cong 10\ \mu m, \text{ respectively } [\delta_{\gamma'}]_{42CrMo4} \cong 6\ \mu m$$

It turns out that for the two steel grades, one unalloyed, the other weakly alloyed, but having close carbon concentrations, the chance of obtaining a nitrided layer composed of a single-phase compound zone ε and a diffusion zone is in favor of the alloy steel. These considerations are determined by the influence of the alloying elements on the isothermal section domains of the Fe-C-N diagram [4].

3.2. The nitrogen and carbon distributions in the nitrided layers

The nitrogen and carbon distribution on the penetration depth represents valuable information for establishing the mechanisms occurring when making nitrided layers. The presence of carbon is supported either by the chemical composition of the steel or by supplementing the working atmosphere containing carbon gaseous components [5]. The glow discharge mass spectrometry analysis (GDMS) is characterized by emission stability, regularity of the erosion speed, high resolution capacity (including that of light elements) and by a continuous quantification on a depth of about 50 μm of the tracked elements concentration profiles. The obtained nitrogen and carbon distribution profiles will be presented in Figs. 1, 2 and 3.

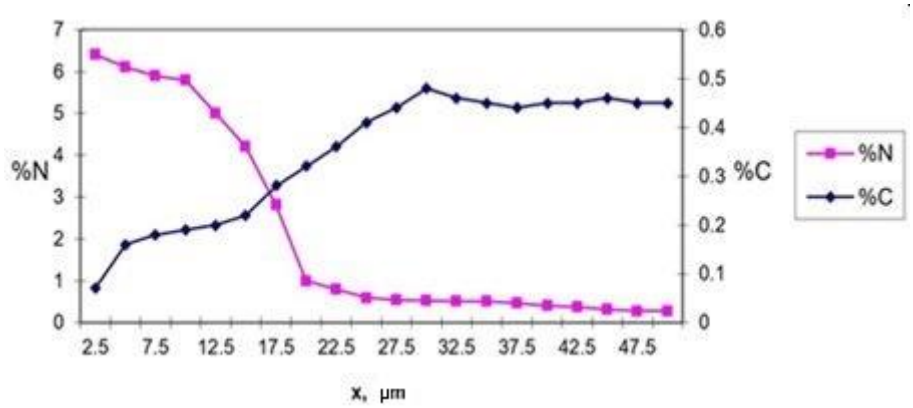

Fig. 1 a. Nitrogen and carbon distribution profiles (GDMS) for sample C1 (C45, T_N=570°C/6h/25%N_2 + 75%H_2).

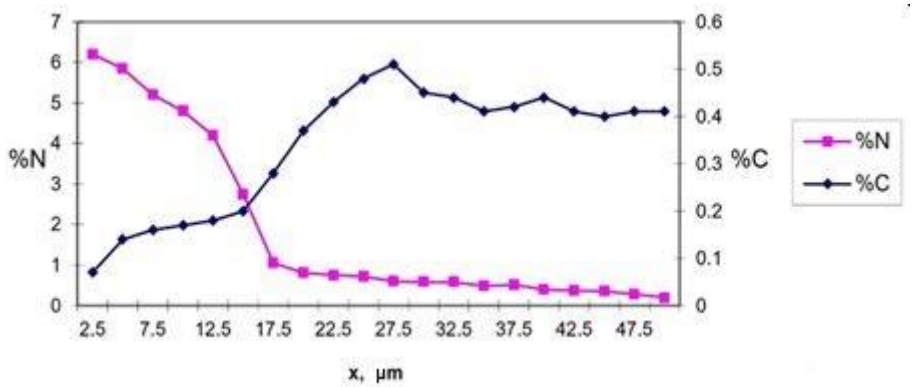

Fig. 1 b. Nitrogen and carbon distribution profiles (GDMS) for sample E1 (42CrMo4, T_N=570°C/6h/25%N_2 + 75%H_2).

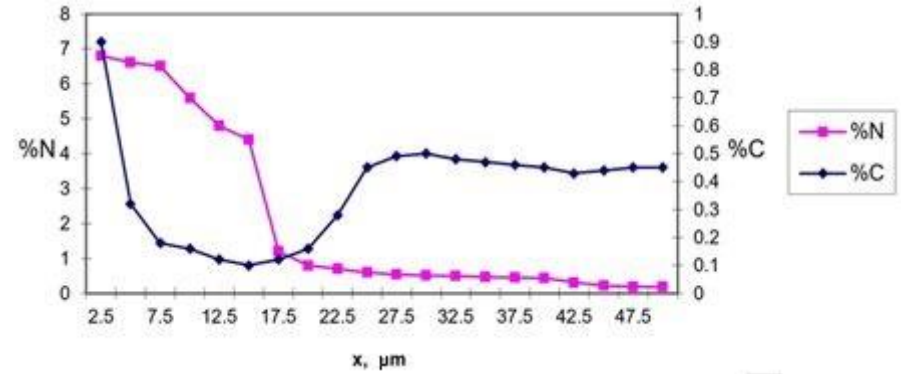

Fig. 2 a. Nitrogen and carbon distribution profiles (GDMS) for sample C2 (C45, T_N=570°C/6h/80%N_2 + 20%H_2).

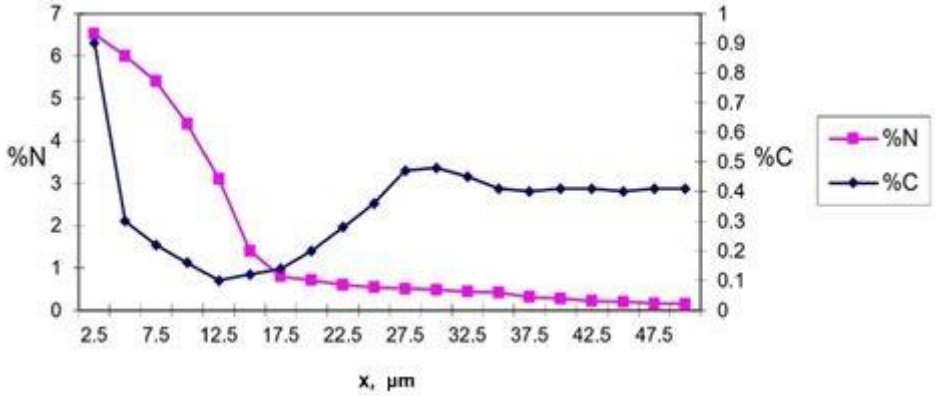

Fig. 2 b. Nitrogen and carbon distribution profiles (GDMS) for sample E2 (42CrMo4,T_N=570°C/6h/80%N_2 + 20%H_2).

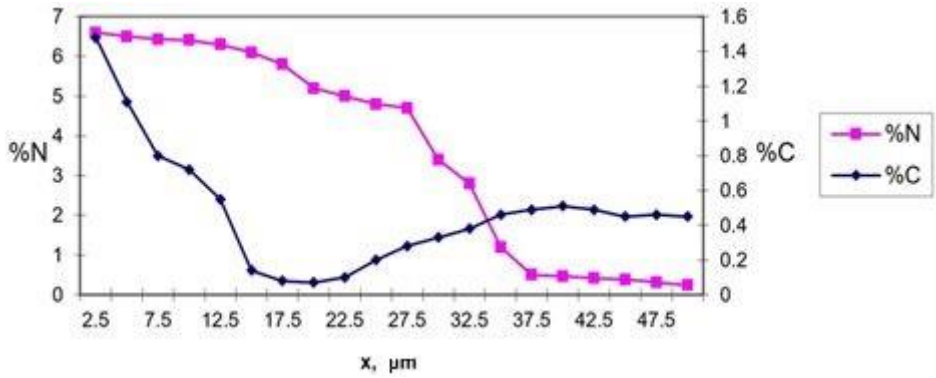

Fig. 3 a. Nitrogen and carbon distribution profiles (GDMS) for sample C3 (C45, T_N=570°C/9h/80%N_2 + 19.5%H_2 + 0.5%CH_4).

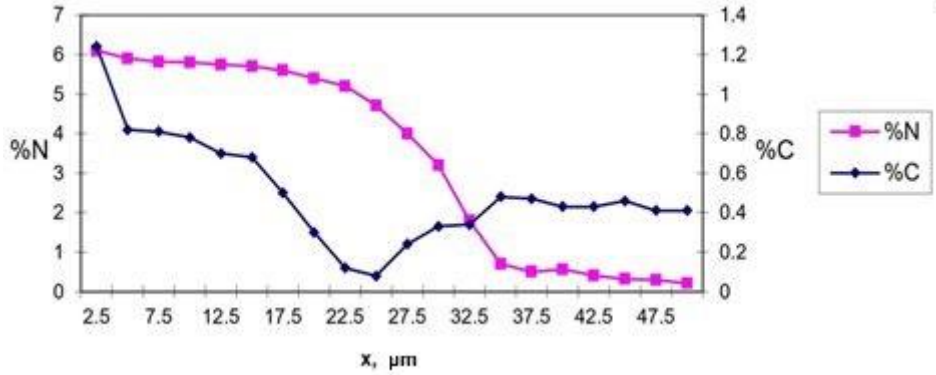

Fig. 3 b. Nitrogen and carbon distribution profiles (GDMS) for sample E3 (42CrMo4,T_N=570°C/9h/80%N_2 + 19.5%H_2 + 0.5%CH_4).

Interpretation of the distribution curves

Generally, the nitrogen distribution profiles obtained by the GDMS method are similar to those constructed analytically. When nitriding is performed below 590°C (the eutectoid temperature) a calculated curve may be obtained [6].

All the theoretical curves are intended for the penetration stage of the active element in the metallic material surface, therefore the saturation stage. The jump present on the distribution curve, which marks the diffusion impossibility in two-phase domains, is not present in the obtained curves. Overall, they are made up of several sections in which the decrease of nitrogen to the depth of the metallic material presents slopes with different angles, characteristic of solid-state transformations that occur during slow cooling. Thus, the jump corresponding to the two - phase domain $\gamma' + \varepsilon$ becomes a curve with a steep slope, given by the solvus lines that borders the mentioned two - phase domain and which, by their specificity, involve secondary phase precipitation [7 - 9].

Once this aspect being overcome, the interpretation of the nitrogen distribution is relevant if informations are associated with those resulting from the carbon distribution aspect. Indeed, its distribution in the nitrided layer follows a more unusual course. However, knowing its different solubility in the phases of Fe-N system, one can justify this profile along the layer's depth. Moreover, the two distribution curves represent an useful source of information regarding the phase structure stability along the layer's depth. The results can be confirmed by X-ray diffraction techniques.

Specific aspects revealed by the nitrogen and carbon distributions in the nitrided layers obtained with regime 1*(samples C1 - C45 and E1 - 42CrMo4)*

- on the depth of the first 10 μm for both materials the nitrogen presents a slightly decreasing distribution, established between 6.4% and 5.9% N (C1), respectively 6.2% and 5.2% (E1). One can mention that the first determination is recorded at 2.5 μm beneath the surface. Regarding the carbon distribution, values well below the average one were determined by the initial chemical analysis. For both samples, from near zero values found at the surface (0.04%C), the slightly ascending distribution reaches only 0.17...0.19% C at 10 μm distance from the surface. It was established that the mentioned composition values correspond to the γ' phase, by analyzing them in parallel. Associating this information with the fact that the white layer, determined by previous measurements, recorded values of 8 ... 10 μm, one may anticipate before the X-ray investigations that its structure will be (predominantly) formed by the γ' phase.
- for the next 40 μm there is a progressive decrease of the nitrogen towards the material inner zone, while the carbon, immediately below the compound area (below the first 10 μm) will show a rather marked increase, recording

even a maximum point at 0.48...0.50% C that corresponds to 20...25 μm depth from the surface. After this point, the value stabilizes to that corresponding to the steel composition (0.43...0.46% for C45, 0.39...0.41% for 42CrMo4).

Specific aspects revealed by the nitrogen and carbon distributions in the nitrided layers obtained with regime 2*(samples C2 - C45 and E2 - 42CrMo4)*

- along the first 10 μm of the layer's depth, the nitrogen distribution is similar to the one previously analyzed. The maximum values measured at the surface, however, reach slightly higher values, 6.8% N for sample C, 6.52% N for sample E. Then again carbon shows a different distribution: from values reaching 0.9% in the surface a sharp decrease follows, up to a distance of 3...5 μm from the reference position where it shows values of 0.17% (sample C) and 0.15% (sample E) that remain constant for the next 7...8 μm. Analyzing once again the composition values, one may identify along the first 3...5 μm an εstructure (the higher solubility of carbon in this phase associated with a higher nitrogen content, but still below the equilibrium value indicated by the Fe-N diagram, justify our assumptions). Further on, for the next 6...8 μm, the analyzed values, in agreement with the previous results, support the existence of a γ' structure.
- for the next 40 μm nitrogen and carbon distributions follow the same path as in the previous situation.

Specific aspects revealed by the nitrogen and carbon distributions in the nitrided layers obtained with regime 3*(samples C3 - C45 and E3 - 42CrMo4)*

- on the first 25...28 μm of depth (corresponding to the thickness of the white layer established by previous investigations) the distribution curves of nitrogen and carbon register similar aspects to those obtained by applying regime 2. The difference consists in the maximum points values reached both by the nitrogen and carbon concentration. Thus, the descending section corresponding to the nitrogen distribution starts for sample C (C45) from the value of 6.6% N (slightly lower than that obtained in the case of regime 2) and during the 28 μm it reaches a 4.8% N value. Similarly for sample E the maximum value appears at 6.1% N (a lower value than that of the equivalent sample obtained by regime 2). The minimum point at the end of the 25 μm of depth is 4.71% N. In terms of carbon distribution, its maximum value exceeds by far the already analyzed levels. For both C and E samples, the maximum carbon values are of 1.48% and 1.24%, respectively. By special techniques of quantitative metallography, the εphase was identified and measured, its thickness is 15 μm for samples C (C45) and even 14 μm for

samples E (42CrMo4). The next subzone, examined on a distance of 5...7 μm, according to the distribution profiles, corresponds to the γ' structure.

- for the next 25 μm (up to the device resolution limit value of max. 50 μm) the distribution of nitrogen and carbon falls within the known configurations.

3.3. Structural information obtained by diffractometric analysis

The identification of the phase constitution of the compounds layer by X-ray diffraction techniques is the most suitable method of investigation. An incident radiation with a small penetration depth was chosen. Thus, radiation with $\lambda_{Cu_{K\alpha}}$ = 1.54 Å wavelength and a data capture depth of ~ 4 μm was used [10]. Sequential depth analysis was performed only in the situation of samples resulted by the application of regime 3, when the combination area actually showed a greater thickness (20...25 μm). XRD analyses at 8 μm and 10 μm depth, respectively, were performed after electrolytical polishing of the superficial layer [11]. Figs. 4, 5 and 6 show the indexed diffractograms of the 6 samples resulted by applying regimes 1 - 3.

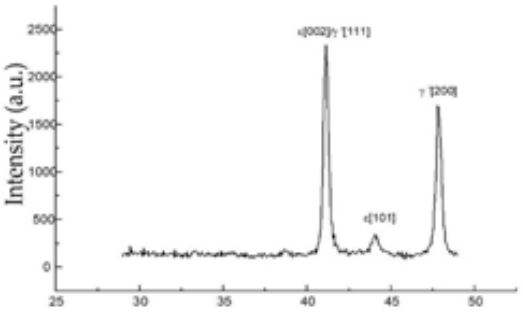

Fig. 4 a. XRD pattern of the C1 sample (C45; 570°C/6h/25%N_2 + 75%H_2) – surface analysis.

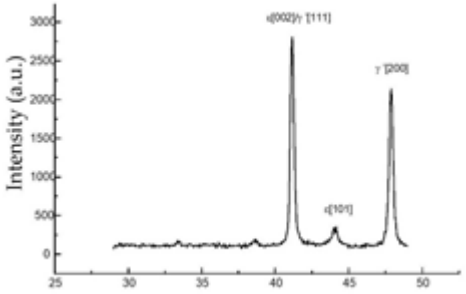

Fig. 4 b. XRD pattern of the E1 sample (42CrMo4; 570°C/6h/25%N_2 + 75%H_2) – surface analysis.

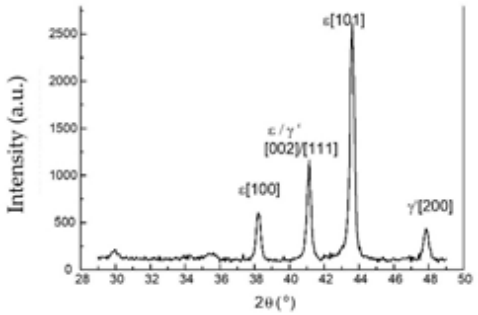

Fig. 5 a. XRD pattern of the C2 sample (C45; 570°C/6h/80%N_2 + 20%H_2) – surface analysis.

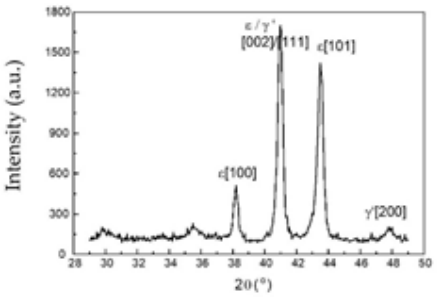

Fig. 5 b.XRD pattern of the E2 sample (42CrMo4; 570°C/6h/80%N_2 + 20%H_2) – surface analysis.

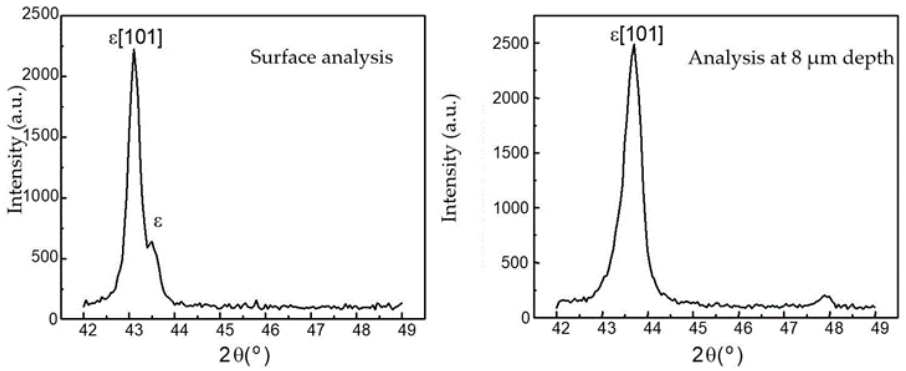

Fig.6 a. XRD pattern of the C3 sample (C45; 570°C/9h/80%N_2 +19.5%H_2 + 0.5%CH_4).

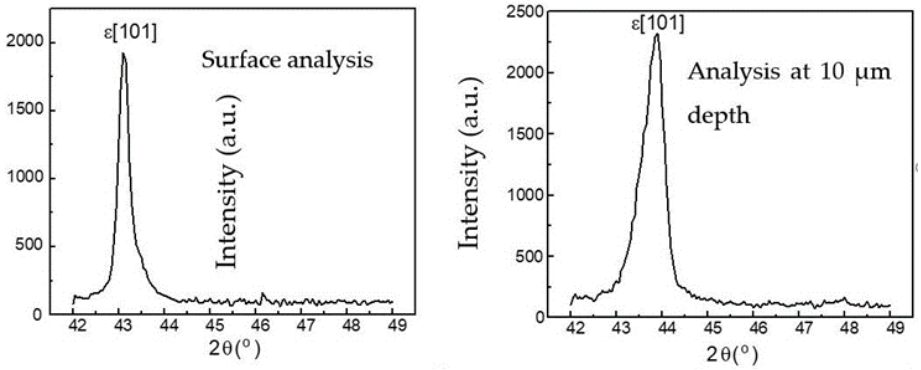

Fig. 6 b. XRD pattern of the E3 sample (42CrMo4 ; 570°C/9h/80%N_2 + 19.5%H_2 + 0.5%CH_4).

Interpretation of diffraction diagrams

The diffractometric analysis revealed the influence of the chemical composition of the working atmosphere on the compounds area phase structure being in direct contact with it. Thus, 3 sets of diffractograms were obtained:

- *for samples C1 and E1 (*atmosphere composition*: 25%N_2 + 75%H_2)*

The diffraction diagrams presented in Fig. 4 *a* and *b* show that the compound area has a two-phase structure $\varepsilon + \gamma'$. The structure is predominantly composed of γ' compound.

- *for samples C2 and E2 (*atmosphere composition*: 80%N_2 + 20%H_2)*

The modification of the gaseous components ratio in the nitriding atmosphere influences the phases proportions in the compound zone, also made up of $\varepsilon + \gamma'$. The ε phase is preponderant.

- *for samples C3 and E3* (atmosphere composition: *80%N_2 + 19.5%H_2 + 0.5%CH_4*)

By adding 0.5% CH_4 to the atmosphere, the compounds layer benefits from indubitable advantages in obtaining a single-phase structure ε, disposed on a

depth as great as possible [7]. The diffraction diagrams performed on the surface, associated with those recorded at a depth of 8 μm(C3) and 10 μm (E3) respectively, support our assertions.

3.4. Structural information obtained by optical microscopy and scanning electronmicroscopy

Structural images were recorded at moderate magnification powers - 500x or even higher - 1000x (scales 20 μm, respectively 10 μm). There are also images taken at higher magnifications, of over 1000x (scales 5 μm and 8 μm), but only taken in the situation when it was necessary to capture more detailed structural features. The etching with the 2% Nital reagent confirms the name of "white layer" assigned to the compound area. For this microstructural region it was necessary to apply a selective etching method [12], consisting of: 2% Nital reagent – 10 s immersion + Vilella reagent - 3...5 s immersion. The method gave satisfactory results only when the compounds area was larger, of over 20 μm. Thus, the separation of the γ' (less chemically resistant, therefore more susceptibile to corrosion) phase from the ε phase was achieved [13]. Another used reagent was the Oberhoffer one. For immersion times that should not exceed 12...15 s and by using special oblique light techniques of optical microscopy, the nitride networks of the alloying elements disposed at grain boundaries were highlighted. Figs. 7, 8 and 9 show layer images of ion nitrided samples C (C45) and E (42CrMo4) according to regimes 1 - 3.

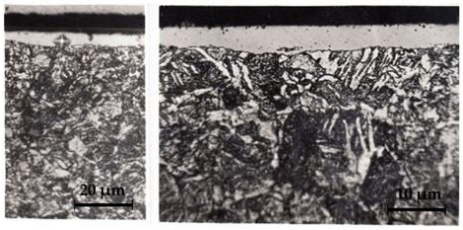

Fig. 7 a. Microstructure of the nitrided layer for sample C1 *(C45, 570°C/6h/25% N_2 + 75% H_2)*. Reagent: Nital 2%.

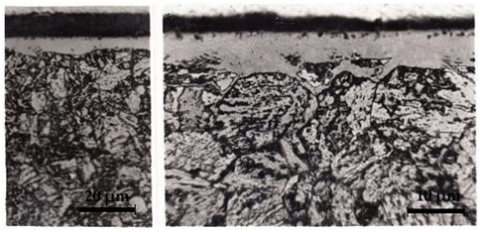

Fig. 7 b. Microstructure of the nitrided layer for sample E1 *(42CrMo4, 570°C/6h/25% N_2 + 75% H_2)*. Reagent: Nital 2%.

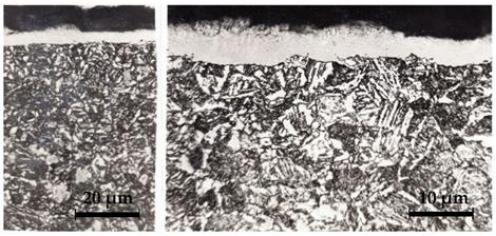

Fig. 8 a. Microstructure of the nitrided layer for sample *C2* (*C45, 570°C/6h/25% N_2 + 75% H_2*). Reagent: Nital *2%*.

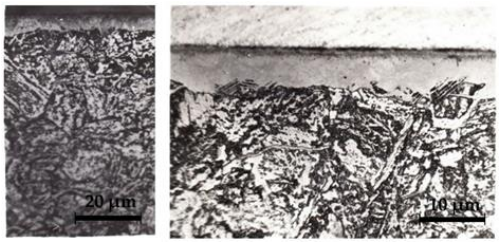

Fig. 8 b. Microstructure of the nitrided layer for sample *E2* (*42CrMo4, 570°C/6h/25% N_2 + 75% H_2*). Reagent: Nital 2%.

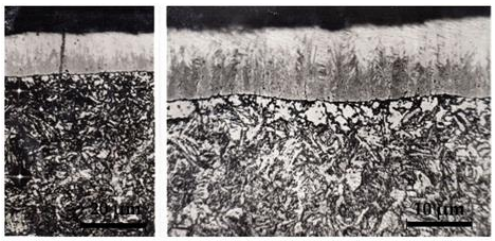

Fig. 9 a. Microstructure of the nitrided layer for sample *C3* (*C45*, *570°C/9h/80% N_2 + 19.5% H_2 + 0.5% CH_4*). Reagent: Nital 2% - 15 s + Vilella - 5 s.

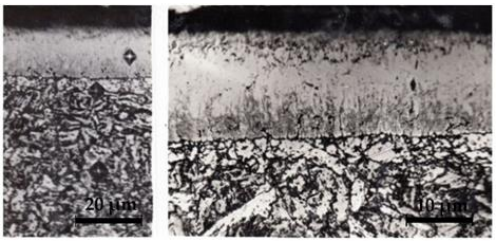

Fig. 9 b. Microstructure of the nitrided layer for sample *E3* (*42CrMo4*, *570°C/9h/80% N_2 + 19.5% H_2 + 0.5% CH_4*). Reagent: Nital 2% - 15 s + Vilella - 5 s.

Interpretation of optical micrographs and scanning electron micrographs

3.4.1. Interpretation of optical micrographs

Microstructures of samples C1 (C45) and E1 (42CrMo4) - Figs. 7 a and 7 b

The microstructure images recorded at 500x magnification show a continuous and uniform compounds zone, with the same morphological characteristics for both samples. One may notice in the 1000x magnification micrographs small discontinuities as a regular pore dispersion at the top of the white layer. These morphological characteristics reveal the existence of the ε phase. The low degree of porosity represents a landmark that the phase is present in a small proportion, most of the white layer being of γ' nature. The rather narrow thickness of the compound area (8...11 μm) did not allow a clear separation of the two phases by applying the selective etching technique. However, one may argue that the majority phase is γ', a hypothesis that is confirmed by the results obtained from diffractometric analysis (XRD) and quantitative chemical composition analysis (GDMS).

By examining the diffusion area at 1000x magnification, one may distinguish in sample micrograph E (42CrMo4) discontinuous networks being well-contoured, uniform, thick and uniformly distributed, approximately parallel to the surface. They do not affect the layer properties, on the contrary, they lead to increased mechanical performances. The "network" morphology represents an indication that there are nitrides of the alloying elements (in this case chromium – based) separated towards the end of the thermochemical treatment holding time. The network thus highlighted and less corroded by the reagent appears bright, slightly embossed, bordering the grain boundary around which it was formed [14].

The acicular morphology, specific to the iron-based nitrides (γ' type), can be highlighted in both the diffusion zone of sampleE1 (42CrMo4) and that of sampleC1 (C45). The essential condition is that the investigation is to be also carried out at high resolution powers. Such nitrides will be identified in micrographs presented in Figs. 10 (a) and (b).

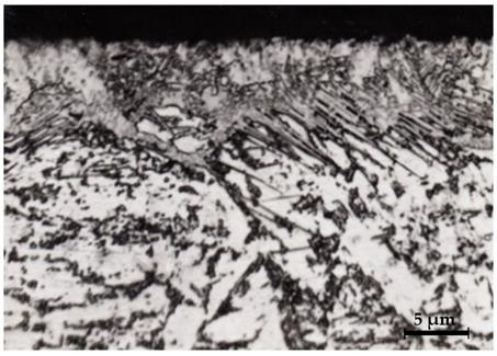

Fig. 10 a. Optical micrograph of the diffusionsau compoun zone (adjacent area of the compounds zone – another field) for sample *E1*. Reagent: Oberhoffer, 5...7 s.

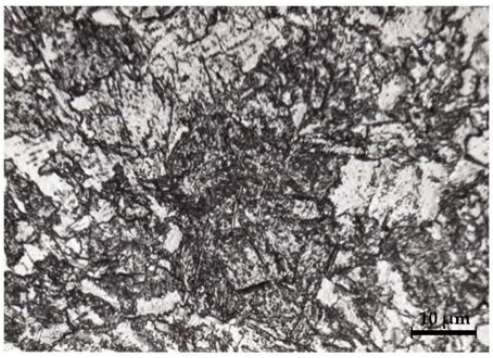

Fig. 10 b. Optical micrograph of the diffusion zone for sample *C1*. Reagent: Nital *2%*.

In micrograph 10 (a) a very heavy precipitation of acicular nitrides γ' are detected within the area adjacent to the compoundszone. The carbon content is still below the average limit, thus favorable to the γ' phase formation. In Fig. 10 (b) micrograph, which records a region within the diffusion zone of sample C1 (C45), no nitride networks are reported but only acicular nitrides, characteristic signals of the γ' phase obtained by precipitation during slow cooling.

Microstructures of samples C2 (C45) and E2 (42CrMo4) – Fig. 8 a and 8 b

The white layer in the presented microstructures has a two-phase structure, which can be established by examining the micrographs performed at 1000x magnification. A higher porosity in the upper areas shows a higher proportion of the phase ε. Even by using the 2% Nital reagent, brighter microconstituents (phase ε) can be distinguished, alternating with darker ones (phase γ'). As seen in Fig. 11, the grains are columnar, suggesting that growth processes are controlled at the interface. Changing the nitrogen - hydrogen ratio (4/1) in the working atmosphere is the main factor that argues for increasing the εphase proportion. The formation of the diffusion zone does not seem to be influenced by the N_2/H_2 ratio. However, nitride precipitates in the area adjacent to the white layer are denser: those that adopt a network - like morphology are more branched, those in acicular form are more abundant. The micrograph seen in Fig. 11 of sample E2 (42CrMo4) captures both aspects.

Fig. 11. Optical micrograph of the diffusion zone for sample E2. Reagent: Nital 2%.

Microstructures of samples C3 (C45) and E3 (42CrMo4) – Fig. 9 a and 9 b

The method of selective etching led to separation of the two phases that make up the compounds layer. Thus, the luminous zone with pores belongs to εphase, while the darker area to γ' phase.

The columnar growth of the two constitutive phases, very evident in the case of γ' phase, is reconfirmed. Dimensionally speaking, ε phase is obviously larger than γ' phase [15]. Therefore, the objective of choosing a working atmosphere of a certain chemical composition in order to stimulate the formation of the εphase has been achieved.

Comparing the thickness of the subzone γ' for both samples (C and E), one can find that it is narrower when formed on an alloy steel substrate. The direct microscope measurements confirm our observations:

$$\delta_{\gamma'}^{C45} = 10...12\ \mu m; \qquad \delta_{\gamma'}^{42CrMo4} = 6...8\ \mu m$$

The influence of the alloying elements is diminished, decreasing the forming tendency of γ' phase in favor of ε phase. One can therefore conclude that a nitride layer with the compound zone predominantly formed by ε + *diffusion zone* has much more favorable formation conditions if the steel is alloyed.

3.4.2. Structural information obtained by scanning electron microscopy

In the following the series of scanning electron micrographs together with their interpretations will be presented.

Scanning electron micrographs of samples C2 (C45) and E2 (42CrMo4)

Fig. 12 a. Scanning electron micrograph of a whole area in sample *C2* (*C45*).

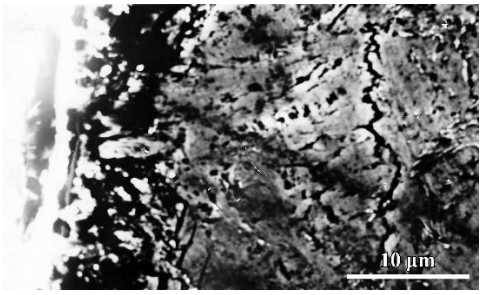

Fig. 12 b. Scanning electron micrograph of a whole area in sample *E2* (*42CrMo4*).

The compounds layer of the $\varepsilon + \gamma'$structure (atmosphere 80% N_2 + 20% H_2) appears distinctly in both micrographs, Figs. 12 (a) and (b). A light, narrow outer sub-area (thickness 2.5 ... 3 µm) is seen, of ε structure followed by a columnar morphology sub-area, with alternating grains of ε (light) and γ' (dark ones) structure. A detailed image of the compounds zone is seen in Fig. 13.

In the diffusion zone, on a typical sorbitic morphology background (with a higher spheroidization tendency in the micrograph of the C- C45- sample), γ' acicular precipitate (sample C- C45) or those with network-like morphology of the alloying elements nitrides (E- 42CrMo4) may be observed. The image in Fig. 12 (b) captures the stage at which the precipitates are at the beginning of their fragmentation. As for the γ' acicular precipitates, in the diffusion zone of sample C (C45) a significant region was detected (Fig. 14).

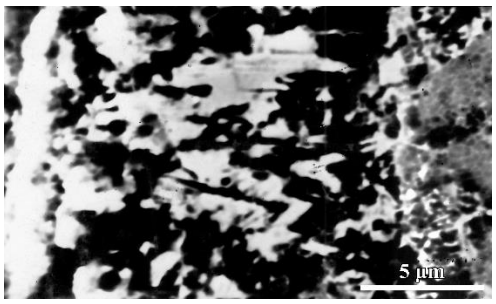

Fig. 13. Scanning electron micrograph of sample *C2* (*C45*) – detailed image of the compounds zone.

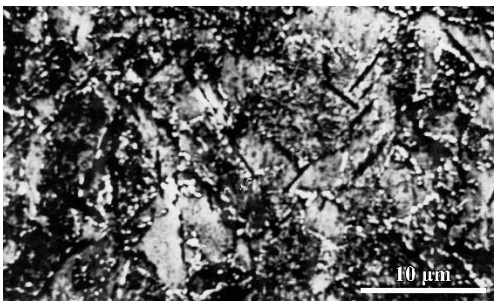

Fig. 14. Scanning electron micrograph of sample *C2* (*C45*)- detailed image of the diffusion zone.

In the Fig. 14 micrograph one may find an abundant precipitation of the γ' acicular nitrides with random orientations, having an average particle length of 4 ... 5 µm.

Scanning electron micrographs of samples C3 (C45) and E3 (42CrMo4)

In these micrographs the research will focus on the compounds area.

Fig. 15 a. Scanning electron micrograph of a whole area in sample *C3* (*C45*).

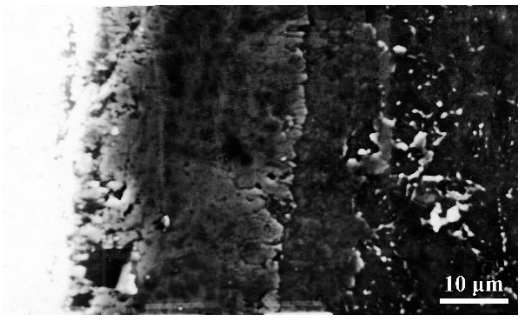

Fig. 15 b. Scanning electron micrograph of a whole area in sample *E3* (*42CrMo4*).

The compound layer is mainly consisting in ε phase [14]. It is porous, with a pronounced porosity tendency towards the outer areas. When comparing the two micrographs, one may observe the increased layer depth of ε phase, in the situation of its formation in a carbon steel (Fig. 16 a). The porosities exhibit mostly a capillary morphology. They play the role of a "lubricant tank", thus reducing the friction coefficient in service [15]. A detail of Fig. 15 (a) scanning electron micrograph, focused on this feature, is shown in Fig. 16.

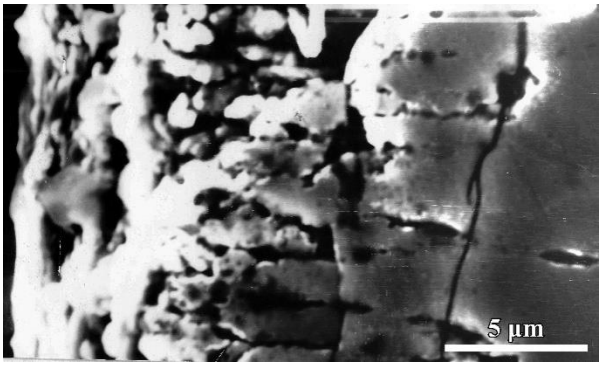

Fig. 16. Scanning electron micrograph of sample C3 (C45) – detailed image of the compounds zone.

In contrast, the γ' phase maximum thickness will be observed in the non-alloy steel structure (fibrous, columnar grain structure) seen in Fig. 15 (b). When compared, a more pronounced porosity of the ε phase formed in the C45 steel will be also noticed [12, 14].

4. Conclusions

Low nitrogen content in the working chamber (*5%N_2 + 95%H_2*) completely suppresses the compounds layer formation, while an average nitrogen content (*20...30%N_2 + 80...70%H_2*) facilitates the formation of a mainly γ' structure. Contrariwise, a high nitrogen content (*80%N_2 + 20%H_2*) makes possible the existence of a biphasic $\varepsilon + \gamma'$ compound layer (mainly ε). It is important to observe that by plasma nitriding an exclusive ε phase layer can never be obtained. Adding to the first atmosphere a small proportion of carbon component gas *(80%N_2 + 19.5%H_2 + 0.5%CH_4)* a structure consisting in two subzones may result, the external one as an ε structure and the internal one as a γ' structure. A fully ε phase structure of the layer could be achieved only by plasma nitrocarburizing, but it is needed to measure carefully the necessary optimal methane proportion.

Phase γ' is definitely formed under intense decarburization conditions. The maximum carbon content that can be dissolved does not exceed 0.2%C, as found by GDMS techniques. The strong back-diffusion phenomena in which carbon atoms are strongly removed are not unique in plasma nitriding, the existence of carbon-concentrated regions beneath the compound area was also observed on gaseous nitriding, but in plasma nitriding this effect is much stronger.

The alloying elements dissolve into γ', partially substituting the iron atoms. As a result, the interstices in which the nitrogen atoms settle are adjusted thus changing the concentration range in which γ' can exist. Formally, the alloying elements are unfavorable regarding its formation, but creating internal stresses the hardness values are increased and a finer grain size may be observed. The εphase, richer in nitrogen, is formed when the "nitrogen potential" is higher, the cathodic sputtering is less intense, and the carbon content is greater.

A sufficient amount of carbon in the atmosphere stimulates its formation and a smaller amount of nitrogen will be dissolved. This effect is beneficial, ε carbonitride has superior mechanical properties as compared to ε nitride: the fragility is diminished and the tribological properties are excellent.

The diffusion area is less influenced by the method (gaseous or plasma nitriding) being directly dependent on nitrogen diffusive transfer. This particularity is provided only by the chemical composition of the steel.

R E F E R E N C E S

1. *T. Lampe, S. Eisenberg andG. Laudien*, Compound layer formation during plasma nitriding and plasma nitrocaburising,*Surf. Eng.*, **vol. 9**, no.1, 1993, pp. 17-28.
2. *E.J. Mittemeijer, W.T.M Straver, P.F.Colijn, P.J. Van der Schaaf andJ.A.Van der Hoeven*, The conversion cementite - ε nitride during the nitriding of Fe-C alloys,*Scripta Metall Mater*, **vol. 14**, no.11, 1980, pp. 1189-1192.
3. *M.E. Bănică, G.G. Grigorescu*, Contributions to the Nitriding Chemical Treatment of a Nitralloy Steel. *U.P.B. Sci. Bull., Series B*, **vol. 71**, no. 3, 2009, pp. 105 – 114.

4. *J. Slicke, L. Sproge andJ. Ågren*, Nitrocarburizing and the ternary Fe-C-N phase diagram. *Scand. J. Metall*., **vol. 17**, no. 3, 1988, pp. 122 - 126.
5. *J. Alphonsa, S. Mukherjee, V.S. Raja*, Study of plasma nitriding andnitrocarburising of AISI 430F stainless steel for high hardness and corrosion resistance, CORROS ENG SCI TECHN,**vol. 53**, no. suppl.1, 2018, pp. 51-58.
6. *T. Dulămiță, E. Florian*, Tratamente termice și termochimice (Heat treatments and thermochemical treatments), Editura Didactică și Pedagogică, București, 1982, p. 373.
7. *C. Ruset, A. Bloyceand T. Bell*, Plasma nitrocarburising with nitrogen, hydrogen and hydrogen sulphide gas mixtures, *Surf. Eng.*, **vol. 11**,no. 4, 1995, pp. 308 - 314.
8. *E. Haruman, T.Bell and Y. Sun*, Compound layer characteristics resulting from plasma nitrocarburising in atmospheres containing carbon dioxide gas additions, *Surf. Eng.*,**vol. 8**,no. 4, 1992, pp. 275-282.
9. *E.J. Mittemeijerand J.I. Slycke*, Thermodynamical activities of nitrogen and carbon imposed by gazeous nitriding and nitrocarburizing atmospheres,*Heat Treat. Met.*, **vol. 23**,no. 3, 1996, pp. 67 – 71.
10. *E. Menthe, K. Rie, J.Schultze and S.Simson*, Structure and properties of plasma nitrided stainless steel, *Surf. Coat. Tech.*,**vol.74–75**, part 1, 1995, pp. 412-416.
11. *J.O.P. Neto, R.O. Da Silva, E.H. Da Silva, J.A. Moreto, R.M. Bandeira, M.D. Manfrinato, L.S. Rossino*, Wear and Corrosion Study of Plasma Nitriding F53 Super duplex Stainless Steel, Mat. Res., **vol. 19**, no. 6, 2016, pp. 1241-1252.
12. *L. Sproge and J.I.Slycke*, Control of the compound layer structure in gazeous nitrocarburising, *Journal of Heat Treating*, no. 9, 1992, pp. 105 – 112.
13. *D. Kovacs, I. Quintana, J. Dobranszky*, Effects of Different Variants of Plasma Nitridingon the Properties of the Nitrided Layer, J MATER ENG PERFORM, **vol. 28**, 2019, pp. 5485–5493.
14. *T. Lampe, S. EisenbergandG. Laudien*, Compound layer formation during plasma nitriding and plasma nitrocarburising. *Surf. Eng.*, **vol.9**,no. 1, 1993, pp. 69-76.
15. *P. Kuppuraj, S. Gunasekaran, P. Puliarasan*, Plasma (Ion) Nitriding of Low Alloy Steel (EN19 grade) and Investigation of Its Physico-Mechanical Properties, International Journal of Science, Technology and Humanities, no. 1, 2014, pp. 93 – 98.